

Central Lancashire Online Knowledge (CLoK)

Title	Towards identifying potent new hits for glioblastoma
Type	Article
URL	https://clock.uclan.ac.uk/24364/
DOI	https://doi.org/10.1039/C8MD00436F
Date	2018
Citation	Sherer, Christopher, Prabhu, Saurabh, Adams, David R, Hayes, Joseph, Rowther, Farzana, Tolaymat, Ibrahim, Warr, Tracy and Snape, Timothy James (2018) Towards identifying potent new hits for glioblastoma. <i>MedChemComm</i> , 9 (11). pp. 1850-1861. ISSN 2040-2503
Creators	Sherer, Christopher, Prabhu, Saurabh, Adams, David R, Hayes, Joseph, Rowther, Farzana, Tolaymat, Ibrahim, Warr, Tracy and Snape, Timothy James

It is advisable to refer to the publisher's version if you intend to cite from the work.
<https://doi.org/10.1039/C8MD00436F>

For information about Research at UCLan please go to <http://www.uclan.ac.uk/research/>

All outputs in CLoK are protected by Intellectual Property Rights law, including Copyright law. Copyright, IPR and Moral Rights for the works on this site are retained by the individual authors and/or other copyright owners. Terms and conditions for use of this material are defined in the <http://clock.uclan.ac.uk/policies/>

Towards Identifying Potent New Hits for Glioblastoma

Chris Sherer,[‡] Saurabh Prabhu,[#] David Adams,[§] Joseph Hayes,[†] Farzana Rowther,[‡] Ibrahim Tolaymat,[⊥] Tracy Warr[‡] and Timothy J. Snape^{,§}*

[‡] Present address: Syntor Fine Chemicals Ltd., Runcorn, Cheshire, WA7 1SR, UK. [#] School of Pharmacy, University of East Anglia, Norwich Research Park, Norwich NR4 7TJ, UK. [§] School of Pharmacy and Biomedical Sciences, University of Central Lancashire, Preston, Lancashire, PR1 2HE, UK. [†] School of Physical Sciences and Computing, University of Central Lancashire, Preston, Lancashire, PR1 2HE, UK. [⊥] Faculty of Medical Science, Anglia Ruskin University, Bishop Hall Lane, Chelmsford, Essex, CM1 1SQ, UK. [‡] Brain Tumour Research Centre, University of Wolverhampton, Wulfruna Street, Wolverhampton, WV1 1LY, UK.

KEY WORDS – scaffold; glioblastoma; cancer; SAR; similarity screening

ABSTRACT – Glioblastoma is a devastating disease of the brain and is the most common malignant primary brain tumour in adults. The prognosis for patients is very poor with median time of survival after diagnosis measured in months, due in part to the tumours being highly aggressive and often resistant to chemotherapies. Alongside the ongoing research to identify key factors involved in tumour progression in glioblastoma, medicinal chemistry approaches must also be used in order to rapidly establish new and better treatments for brain tumour patients. Using a computational similarity search of the ZINC database, alongside traditional analogue design by medicinal chemistry intuition to improve the breadth of chemical space under consideration, six new hit compounds (**14**, **16**, **18**, **19**, **20** and **22**) were identified possessing low micromolar activity against both established cell lines (U87MG and U251MG) and patient-derived cell cultures (IN1472, IN1528 and IN1760). Each of these scaffolds provides a new platform for future

development of a new therapy in this area, with particular promise shown against glioblastoma subtypes that are resistant to conventional chemotherapeutic agents.

Introduction

Glioblastoma are the most common form of malignant brain tumours in adults and account for 12-15% of all primary intracranial neoplasms, and as aggressive cancers, are often resistant to treatment. The median survival time is 6 months overall with only 28% of glioblastoma patients surviving for more than one year, and only 3% of patients surviving more than three years.¹ Whilst the prognosis for patients is generally very poor, the best standard treatment is currently surgical resection followed by concomitant radiotherapy to the resection site and chemotherapy with temozolomide (Figure 1), in the so-called Stupp protocol.² Unfortunately, such a demanding treatment regime only leads to a mean survival of 14.6 months and a two year survival of 26.5%, statistics which highlight that crucial investment is needed in the search for improved treatments, not only to improve survival times *per se*, but to improve survival along with a better quality of life.

Our initial studies in this area demonstrated that certain 2-arylindoles (e.g. **1** and **2**, Figure 1) have anti-glioblastoma activity.³ In the case of **1**, the mechanism of this activity is consistent with the generation of reactive oxygen species (ROS) followed by autophagic cell death, which in some cases gave low micromolar EC₅₀ values against patient-derived short-term cell cultures.^{3, 4} The research described herein expands on our previous programme of work and leads to the discovery of new and possibly improved scaffolds for further development into much needed glioblastoma treatments. Bond dissociation enthalpies (BDEs) were calculated using density functional theory (DFT), as a widely used parameter to measure the ease and stability of radical formation for a species, in an attempt to rationalise the structure-activity relationships in terms of a ROS mechanism.⁵⁻⁷

The innate heterogeneity of glioblastoma is well-documented with individual tumours harbouring a wide spectrum of different genetic abnormalities.^{8, 9} This molecular diversity accounts

for the differential efficacy of cytotoxic agents in glioblastoma patients; for example, mutation of the *TP53* tumour suppressor gene and hypermethylation the DNA repair gene *MGMT*, are associated with increased sensitivity to drugs such as CCNU, temozolomide and vincristine.¹⁰⁻¹²

In the present study, the anti-tumour activity of compounds were assessed in 5 glioblastoma cell cultures comprising 2 established cell lines (U87MG and U251MG) and 3 patient-derived short-term cell cultures (IN1472, IN1528 and IN1760). U87MG and IN1760 were *TP53* wild-type whilst the remaining 3 cultures harboured various *TP53* mutations. Methylation and transcriptional silencing of *MGMT* was present in 3 cultures (U87MG, U251MG and IN1760).¹³ In previous studies, we have determined the differential responses of these cultures to a number of chemotherapeutic compounds which act through diverse mechanisms. In all cases, IN1760 and IN1472 are the most resistant and sensitive cultures respectively, with the remaining 3 cultures demonstrating an intermediate response.¹⁴

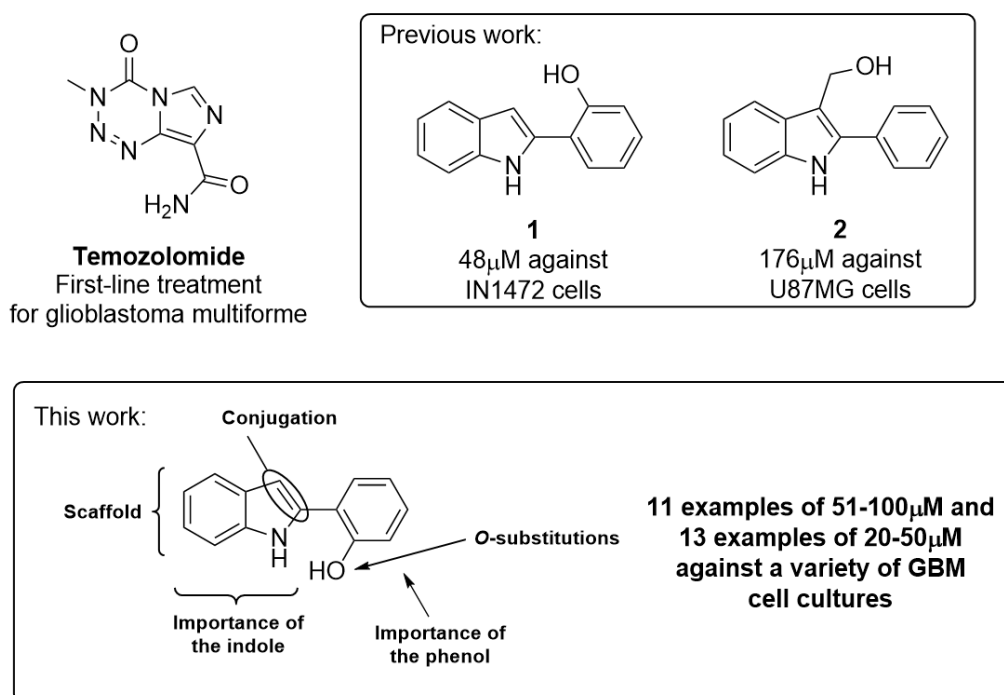


Figure 1. Structure of the first-line treatment temozolomide for malignant brain tumours of the type glioblastoma multiforme (GBM), and two 2-aryl indoles from our previous work on anti-glioblastoma lead compounds.³ The work described herein is depicted by the box entitled 'This work' showing the features of **1** that were studied and some selected EC₅₀ values.

Figure 1 outlines our approach towards the investigation of structure-activity relationships between this known class of compound (**1**) and its anti-glioblastoma activity. Due to the inherently non-exhaustive search of chemical space in our approach, one would not necessarily expect to find a compound with exceptional activity but one may expect to find an uncommon fragment, or a fragment with development potential, with reasonable activity for further development. This further development could then take the shape of a more traditional structure-activity relationship based approach, thus allowing the investigation of the more local chemical space of the active drug fragment.¹⁵

Results and Discussion

Exploring the 2-phenylindole core of lead compound **1**

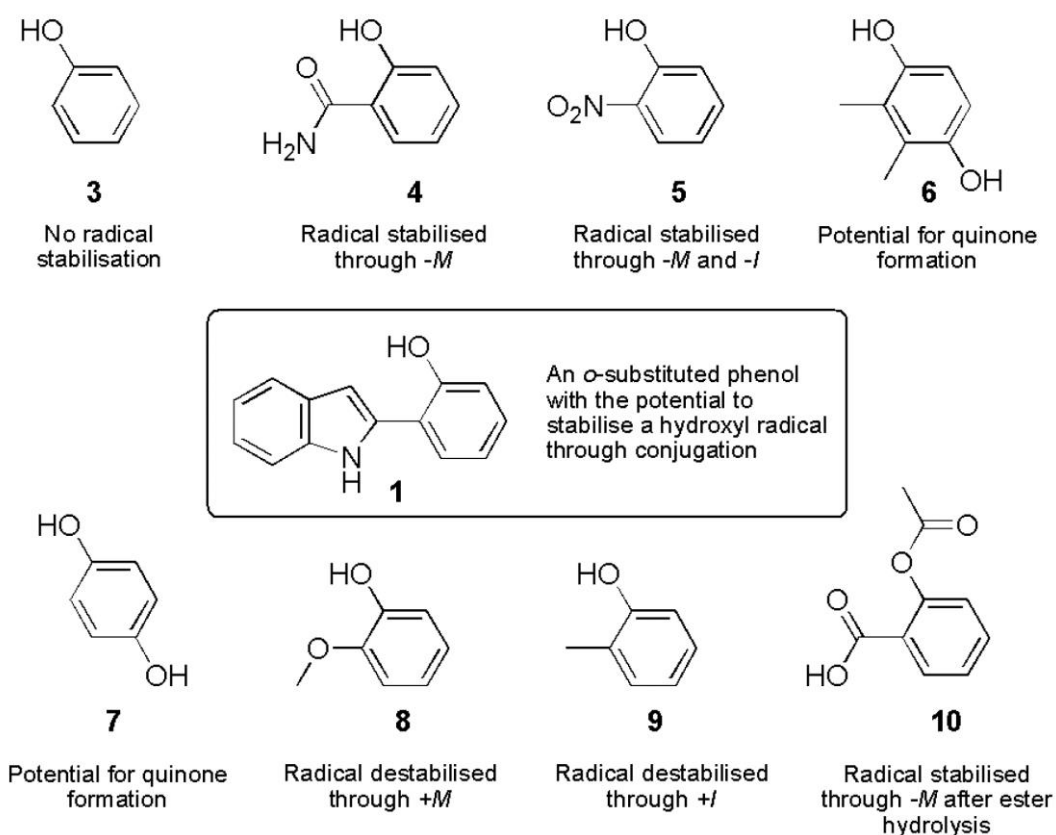


Figure 2. The series of phenols tested in order to establish the importance of the indole group. **10** is assumed to hydrolyse to the phenol in the cell. *M* and *I* represent mesomeric and inductive effects, respectively.

While there are many examples of complex phenols, polyphenols and hydroquinones having reasonable anti-proliferative activity,¹⁶⁻¹⁸ reports on the cytotoxic activities of simple phenols are relatively few in number. Nevertheless, there is some evidence that certain simple phenols do have modest cytotoxic activity, and increasing the complexity of the phenols appears to significantly improve the activity.^{19,20} One of the reasons for the cytotoxic activity of phenolic compounds lies in their ability to generate ROS,²¹ which in turn, relies on their ability to lose both a proton and an electron (formally a hydrogen radical) from the hydroxyl group, subsequently forming both reactive chain-propagating radicals, and a phenoxyl radical.²² Gas phase bond dissociation enthalpies (BDEs) can act as excellent primary indicators of free radical scavenging activity and it has been suggested that trends in BDEs are only weakly solvent dependent,^{5, 23} where DFT calculations have been successfully used to compute O-H BDEs for phenolic compounds.^{5, 24, 25} Calculated BDEs provide a useful predictive measure of the relative ease of ROS formation. We calculated a gas phase BDE of 87.7 kcal/mol for phenol at the B3P86/6-311G**+ level of theory, which is consistent with previous reported calculations of this type when compared with experiment.²⁶ As comparisons between predicted relative BDE values are more accurate within structurally similar series of compounds, we follow suit in our analysis herein.

Based on such precedent, and our previous results confirming the involvement of ROS,³ lead compound **1** can be considered to be an *ortho*-substituted phenol with the indole ring acting as a conjugated system to increase radical stabilisation once formed. With this in mind, a small series of simple, commercially available phenols were screened (Figure 2) to see if mesomeric (*M*) and/or inductive (*I*) effects alone could act in the same way as the indole in terms of affecting activities.

Compound	U87MG	U251MG	IN1472	IN1528	IN1760	BDE (kcal/mol)
1	126 (101, 154)	130 (112, 215)	>625 ^a	99 (85, 191)	185 (87, 630)	77.1
3	834 (717, 968)	1229 (966, 1710)	1731 (1261, 2990)	747 (543, 1203)	>4000 ^a	87.7
4	760 (656, 881)	1205 (889, 1967)	1389 (1156, 1627)	793 (683, 821)	> 4000 ^a	91.6
5	888 (759, 1034)	1251 (994, 1630)	n.d.	890 (699, 1136)	> 4000 ^a	101.1
6	n.d.	17 (15, 20)	n.d.	n.d.	n.d.	79.5
7	n.d.	57 (46, 71)	n.d.	n.d.	n.d.	82.1
8	492 (436, 555)	1141 (993, 1341)	2021 (1296, 5822)	813 (640, 1084)	>4000 ^a	86.8
9	664 (537, 844)	1565 (1172, 3146)	1436 (1255, 1642)	744 (682, 812)	>4000 ^a	85.5
10	723 (539, 1020)	1341 (988, 2202)	1413 (1221, 1728)	787 (648, 983)	>4000 ^a	94.0 ^b

Table 1. Comparison of EC₅₀ values (μ M) between a series of simple phenols (the values in parentheses represent the 95% confidence interval level, 95% CI), together with calculated O-H BDEs at the B3P86/6-311+G** level of theory. n.d. = not determined in this batch. The best EC₅₀ values are highlighted in bold. ^aEC₅₀ not reached. ^bBDE for salicylic acid. EC₅₀ values were calculated using a sulphorhodamine B (SRB) assay and represent anti-proliferative activity.

The activities of this series of simple phenols **3-10** are shown in Table 1 alongside **1** for comparison. Reviewing the activities of the individual phenols against the individual cell cultures (U87MG, U251MG, IN1472, IN1528 and IN1760) generally shows that there isn't much variation in activity, in a broader sense, with only modest activity observed, with the exception of the two hydroquinones (**6** and **7**) against the U251MG cell lines (EC₅₀s = 17 and 57 μ M respectively). Whilst this data suggests that no clear conclusion can be drawn for the relative activities of these phenols and hydroquinones against GBM, hydroquinones are known to be involved in redox cycling in other systems,^{27, 28} and so such compounds warrant further study in the area of brain tumour research. Especially, since it is known that such compounds can be toxic if not-targeted to the tumour site directly, and so further study would focus on finding analogues that could demonstrate selectivity over non-cancerous cells. On the contrary, with the exception this time of U251MG, in general **1** seems to have significantly higher anti-proliferative activity than the phenols against the other four cultures. The magnitude of this difference in activity suggests that, in this context at least, either the *ortho*-indole group is an excellent substituent for the phenol group, or that

there is a unique and perhaps synergistic effect between the indole and phenol moieties. Although there doesn't appear to be a strong correlation between BDE and EC₅₀ (Table 1), the three most active compounds (**1**, **6** and **7**) do have the lowest BDE values of all those tested. The almost complete lack of activity in the IN1760 culture is representative of its extremely resistant nature to chemotherapeutic drugs.

The importance of the phenol group in 1

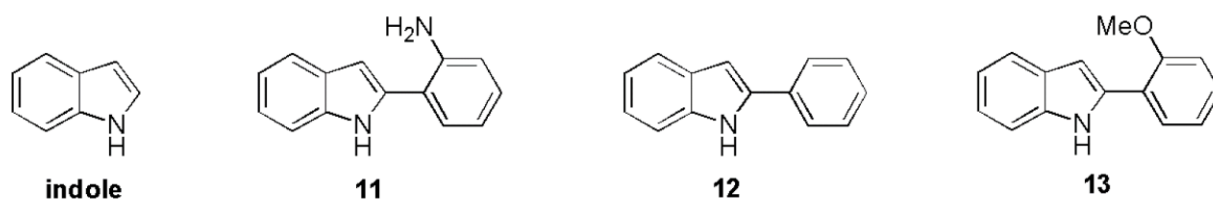


Figure 3. Analogues used to probe the importance of the phenol group.

In order to determine the significance of the phenol group in **1**, a series of closely related analogues (Figure 3) were developed (the synthesis of all compounds prepared can be found in the Supporting Information). These analogues included a compound without the phenol group (indole), an aniline analogue (**11**), a compound without the phenolic-OH group (2-phenylindole, **12**), and a methoxy derivative, **13**.

Compound	U87MG	U251MG	IN1472	IN1528	IN1760	BDE (kcal/mol)
1	126 (101, 154)	130 (112, 215)	>625 ^a	99 (85, 191)	185 (87, 630)	77.1
Indole	>625 ^a	>625 ^a	>625 ^a	>625 ^a	>625 ^a	No BDE
11	257 (82, 525)	328 ^b	155 (82, 828)	153 (59, 256)	n.d.	84.8
12	>625 ^a	>625 ^a	>625 ^a	>625 ^a	>625 ^a	No BDE
13	>625 ^a	n.d.	n.d.	n.d.	n.d.	No BDE

Table 2. Comparison of EC₅₀ values (μM) between **1** and analogues probing the significance of the phenol group (95% CI), together with calculated O-H BDEs at the B3P86/6-311+G** level of theory. The best EC₅₀ values are highlighted in bold. n.d. = not determined in this batch. ^aEC₅₀ not reached. ^bCI not calculable.

This is an interesting data set since the response is broadly similar across cultures, implying that the cytotoxic effects, or lack of, are independent of genetic background. Importantly, upon removal of either the hydroxyl group (analogue **12**), the whole phenolic substituent (indole) or masking it (**13**), the EC₅₀ value rises to above what can be determined under the assay conditions employed (Table 2). Although the extent of activity loss cannot be determined absolutely, it can be confidently asserted that the phenol is essential for activity, yet must be sufficiently substituted to exert its effect (see activity of phenol in Table 1).

When comparing the activity of **1** with its aniline analogue (**11**), across all four cell cultures that they were compared against, **1** has consistently higher activity (with the exception of IN1472), although both compounds have only modest activity, possibly attributed to the fact that only these two compounds have a calculated BDE. Under normal practises, this result would encourage similar analogues of **1** and **11** to be studied, including heteroatom analogues such as indolylthiophenols or indolylphenylphosphines, however, such an in-depth approach was not the focus of the study here.

A Similarity Searching Approach

One of the key steps in the early stage of drug development is finding active hits which can serve as molecules that will be further optimised into potential drug candidates. In order to identify such alternative scaffolds that could potentially act through a similar mechanism, we carried out a computational similarity study, whereby a large database could be interrogated, thus expanding the area of chemical space being explored beyond that which may be familiar to a medicinal chemists, to those which are documented in a curated repository or database. The choice of database is an important one and can strongly influence the results of a similarity search.²⁹ Accordingly, in order to discover otherwise non-obvious structural analogues of our lead compound/fragment (**1**), a similarity search was carried out.

On balance, the most suitable database considered for this work was the ZINC database.³⁰ It is of particular interest since the data is curated into subsets, which can, by judicious selection of the

subsets, improve the efficiency of the search process. In this work, the subset of data that has been opted for was the fragment-like subset of compounds (molecular weight ≤ 250 , $\log P \leq 3.5$, number of rotatable bonds ≤ 5) which were advertised as currently in stock, a subset that included almost 800,000 entries. Similarity screening was conducted on this database using ShaEP (a software tool for a rigid-body superimposition and similarity evaluation of ligand-sized molecules)³¹ but to account for the fact that ShaEP handles structures as rigid bodies, up to three low energy conformations of the compounds were pre-generated using BALLOON,³² producing a total of over 1.4 million structures for interrogation. From preliminary computational calculations, what a medicinal chemist might call very similar from a chemistry perspective (e.g. heteroatom analogues or positional isomers ShaEP would consider to have a similarity of around 0.8. The 105 compounds with the highest overall similarity value were taken forward as a manageable number of hits to be manually inspected in the next step. The structures of these 105 candidate compounds can be seen in the Supporting Information. Upon inspection it became apparent that these 105 compounds could be grouped based on our lead compound (**1**) and its accepted mechanism of action being related to the formation of a phenol radical for ROS generation.³

The first and largest group (59 entries) comprised of compounds that had no way of generating a phenolic (or analogous) radical, for example, compounds that had no phenol or aniline group. Since these compound don't agree with the current evidence on how our lead compound acts,³ they were not included in the work beyond this point. Excluding this class of compounds left a further 46 compounds to be considered.

The next group of compounds were 20 isomers or pseudoisomers of **1**. Unsurprisingly, compounds in this group typically had the highest similarity score (0.79-0.88). However, this work was being done with the intention of encountering analogues which would otherwise not have been considered, by investigating a wider range of chemical space as possible, and so compounds in this group were also not considered further.

The third group of compounds (26 entries, some of which are shown in Figure 4) are those which may be able to form a conjugated radical (like **1**), but have a core other than 2-phenylindole (with the exception of **19** which is included here for comparison). Such a scaffold-hopping approach has been widely applied by medicinal chemists to discover equipotent compounds with novel backbones that have improved properties,¹⁵ and using this approach revealed compounds with the potential for a phenolic-like radical to be formed.

Within this third group, a total of 14 different cores other than the 2-phenylindole core of lead compound **1** were identified (see Supporting Information for structures), with the 2-phenylbenzimidazole core occurring far more than any other.

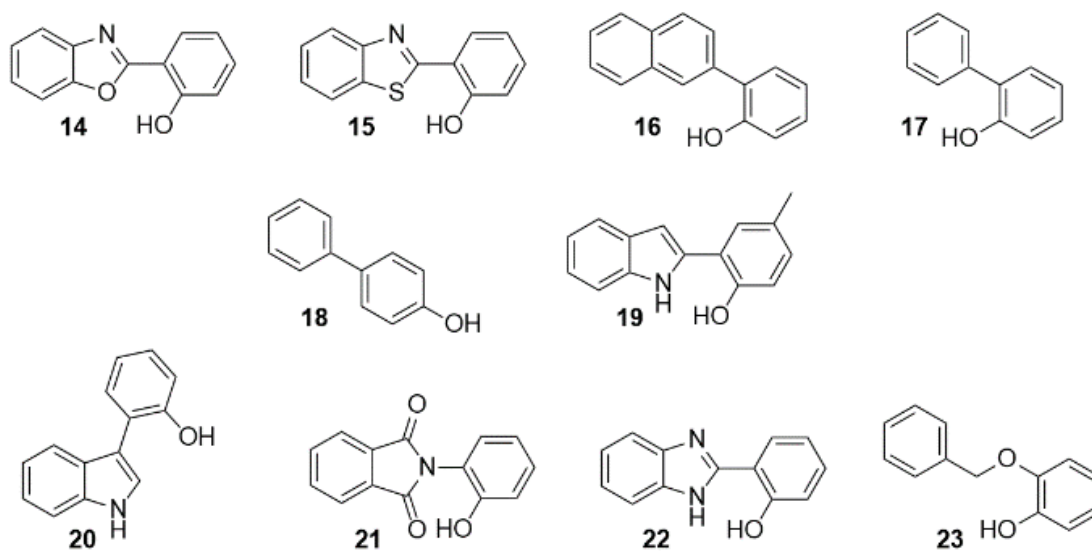


Figure 4. The analogues tested with different scaffolds to that of **1**. EC₅₀s can be seen in Table 3.

The analogues of compound **1** identified were screened for biological activity are shown in Figure 4. The biological data for **14-23** can be seen in Table 3.

Compound	U87MG	U251MG	IN1472	IN1528	IN1760	BDE (kcal/mol)
1	126 (101, 154)	130 (112, 215)	>625 ^b	99 (85, 191)	185 (87, 630)	77.1
14	52 (34, 82)	2257 (1521, 7815)	n.d.	n.d.	>2500 ^b	98.0
15	>1250 ^a	>1250 ^a	>1250 ^a	>1250 ^a	>1250 ^a	92.5
16	48 (37, 62)	92 (83, 101)	n.d.	104 (87, 123)	>1000 ^b	86.6
17	n.d.	372 (290, 412)	n.d.	361 (130, 818)	236 (154, 377)	87.0
18	n.d.	102 (76, 126)	n.d.	85 (66, 111)	81 (70, 130)	85.1
19	n.d.	21 (18, 24)	n.d.	29 (25, 35)	32 (28, 36)	75.6
20	n.d.	95 (81, 113)	n.d.	120 (38, 429)	231 (120, 1002)	82.9
21	n.d.	916 (619, 1925)	n.d.	744 (459, 1642)	1079 ^c	90.0
22	n.d.	23 (19, 27)	n.d.	25 (19, 31)	36 ^c	83.2
23	n.d.	304 (254, 433)	n.d.	193 (87, 848)	371 (216, 858)	85.9

Table 3. Comparison of EC₅₀ values (μM) between compound **1** and a series of analogues with different scaffolds as shown in Figure 4 (95% CI), together with calculated O-H BDEs at the B3P86/6-311+G** level of theory. ^a EC₅₀ not reached as the compound precipitated out of solution >1250 μM . n.d. = not determined in this batch. The best EC₅₀ values are highlighted in bold. ^b EC₅₀ not reached. ^c CI not calculable.

Benzothiazole **15** precipitated out of solution at concentrations greater than 1250 μM and so its EC₅₀ could not be calculated. Whereas, comparing benzoxazole **14** and compound **1** reveals that overall, **1** has higher activity, with the exception of the U87MG cell line. This seems to indicate that the 2-phenylindole core is better than the intuitively highly similar benzoxazole and benzothiazole cores as a molecular scaffold for anti-glioblastoma compounds, at least in these cultures.

Comparing **1** against its naphthalene analogue (**16**) shows that the naphthalene analogue has higher activity against U87MG and U251MG cell cultures, with **1** only having significantly higher activity against IN1760, indicating that the naphthalene analogue appears to be a very active compound (the similarity between **1** and **16** being 0.81). This is significant, as it indicates that the weakly hydrogen bonding NH group of **1** is not essential for activity (a theory supported by the

activity observed with **14** against U87MG cultures), and that the role of the scaffold may be limited to such effects as radical stabilisation, sterics and/or π -stacking.

Comparing **1** against **17** on the three cell cultures studied shows that **1** has superior activity against all. Again, this effect provides evidence that the *ortho*-indole group appears to be an excellent substituent for phenol, as indicated by the data in Table 1.

Interestingly, comparing the activities of **16** and **17** suggests that the extended naphthalene core is beneficial for activity. Similarly, the *para*-phenyl phenol analogue (**18**), highlights possible areas for further study in a more detailed approach to SAR.

Compounds **1** and **20** were chosen for comparison in the hope that these isomers would give information about the importance of shape. As previously revealed, **1** behaves as a ROS generator, the effects of which can be attenuated by the antioxidant ascorbic acid, a feature that is directly linked to the presence of the hydroxyl group.³ In this respect, the electronics of **1** and **20** are expected to be similar, as they have the same number of canonical forms to stabilise the proposed hydroxyl radical (Figure 5). In the event, the compounds were found to have very similar activities against all three cell cultures on which they were compared, with **1** being slightly more active against the IN1528 and IN1760 cultures, and **20** being more active against the U251MG culture.

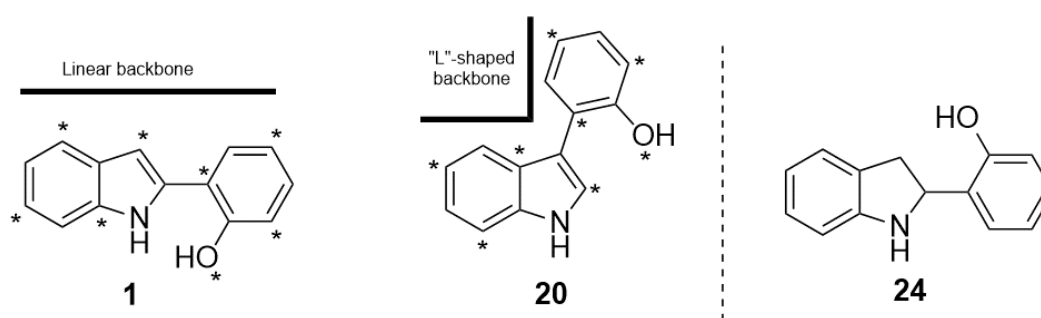


Figure 5. The possible locations of a delocalised phenol radical, identified by an asterisk (*), on **1** and **20** (left); and an analogue of **1** with reduced conjugation, **24** (right).

Surprisingly, indole **19**, which contains a +I methyl group *para* to the hydroxyl, and thus is suitably positioned to stabilise a radical at that position, is extremely active against the short-term

cell cultures. This particular indole is known to scavenge free radicals *in vitro*, albeit at lower concentrations than used here, and so presumably this increased activity when used at higher concentrations is the result of a more toxic, longer-lived radical in the cell.³³

Interestingly, compounds **21** and **22** show drastically different activities. Compound **21** has significantly reduced activity against all three cell cultures, presumably the result of a reduction in radical stabilisation with the non-conjugated phthalimide ring, whereas **22** has very potent activity with values of $EC_{50} \leq 36 \mu\text{M}$ for all three cell cultures and is thus more active than its heteroatom analogues **14** and **15**, as well as compound **1**. All these comparisons indicate that specific scaffolds can have activity against different glioblastoma cell cultures. Even if the observed activity does not occur via the same ROS mechanism, the process of similarity searching has successfully allowed us to identify new hit compounds of higher activity than the lead compound. Structurally speaking, the six new lead compounds **14**, **16**, **18**, **19**, **20** and **22** would appear to be able to support a radical and act through a ROS mechanism (supported by their high activities, Table 3).

Considering all of this data together, it would seem that the activity of **1** is not highly sensitive to three-dimensional shape, as seen with the comparison of **1** and **20**. Furthermore, activity does not seem particularly sensitive to the bicyclic ring system (see compounds **14**, **16**, **18**, **20** and **22**) either; features which we have identified and which has delivered numerous compounds with improved activity compared to **1**. However, perhaps of even greater importance is that new hit compounds have been identified that are very active against the extremely resistant IN1760 culture (compounds **19** and **22**).

Furthermore, compound **23**, found during the similarity search mentioned above, is both chemically and structurally dissimilar to **1**, yet is considered by the ShaEP software to be highly similar in terms of both shape and electronics of the system, with an overall similarity score of 0.785.

However, compound **23** has only modest activity against the cultures studied. Interestingly, however, **23** is much more potent than the related simple phenol guaiacol (**8**) above (EC₅₀ values for U251MG = 1141 μM; IN1528 = 813 μM; and IN1760 = >4000 μM).

In general, again there is no strong correlation between activity and BDE, but the best two compounds identified from the similarity searching approach (**19** and **22**) have two of the lowest BDE values of the new compounds.

Reducing the conjugation of compound 1

In order to investigate the necessity of conjugation between the proposed phenol radical and the indole motif for radical stabilisation, an analogue with reduced conjugation between the two ring systems should be less active if a fully conjugated system is required (**24**, Figure 5). The BDE of **24** was calculated (90.2 kcal/mol) and follows the expected trend compared to the more conjugated **1** (77.1 kcal/mol). In addition to its reduced conjugation, the three-dimensional shape of **24** is somewhat different to that of **1** due to the loss of planarity inherent in reducing the carbon-carbon double bond (sp²→sp³). Nevertheless, as has been shown by the analogues depicted in Figure 4, activity within this phenolic class of compounds is not highly sensitive to shape, so this issue may be moot.

In the event, the EC₅₀ values for **24** were: 122 μM (U251MG); 123 μM (IN1528) and 148 μM (IN1760), with **1** having comparable activities against the patient-derived cell cultures. As a result, determining the superior anti-glioblastoma agent is difficult based solely on this data alone. What can be inferred is that the full conjugation seen in **1**, which was originally considered to be essential for its activity, is perhaps not the only factor involved in promoting activity.

The effect of *O*-protected analogues

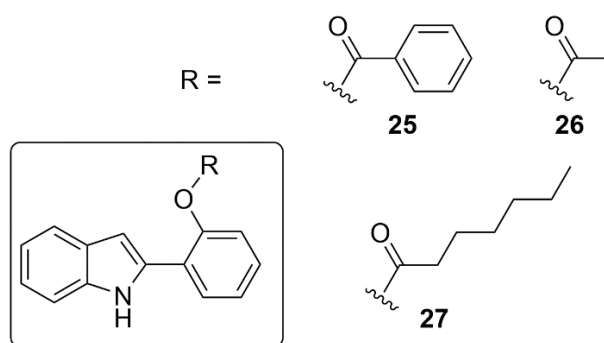


Figure 6. *O*-protected analogues.

In previous work, compound **1** was observed to have a rapid onset of activity (<1h).³ The compounds shown in Figure 6 were prepared and tested to further understand and mitigate this rapid onset of activity of **1**³ by controlling the release of the active compound through a, presumably enzyme-driven, hydrolytic process. The activities of the compounds depicted in Figure 6 are shown in Table 4.

Compound	U251MG	IN1528	IN1760
1	130 (112, 215)	99 (85, 191)	185
25	39 (30, 47)	38 *	n.d.
26	31 (19, 59)	80 (51, 96)	n.d.
27	38 (28, 59)	29 (8, 37)	n.d.

Table 4. Comparison of EC₅₀ values (μM) between **1** and a series of *O*-substituted derivatives (95% CI). n.d. = not determined in this batch. The best EC₅₀ values are highlighted in bold. * CI not calculable.

Interestingly, all three esters have better activity than compound **1** against the U251MG and IN1528 cell cultures, presumably the result of improved cell penetration with the more hydrophobic compounds. However, that the compounds result in similar EC₅₀ values eventually suggests that the esters are hydrolysed, liberating compound **1**.³⁴

To investigate the possibility of the *O*-protected analogues of **1** being used as delayed-release prodrugs, a time course assay for both **1** and its *O*-heptanoyl analogue (**27**) was carried out

on two glioblastoma cell cultures. The results (see Supporting Information) confirmed that compound **1** does have a rapid activity against both cell cultures studied, whereas **27** reduced cell viability much more gradually. Importantly, both compounds tended towards the same activity over 24h. This agrees with the hypothesis that the heptanoyl group can be cleaved off to produce compound **1**, as the activity of compound **27** is ultimately equal to that of compound **1**, yet it takes a measureable time for the enzymatic cleavage to occur. Presumably, a similar unmasking of the phenol group can occur with **13**, this time with enzymes that are capable of demethylation, but based on the activity observed with **13** this either doesn't take place, or is slow.

Conclusion

Five structural features of compound **1** were investigated (Figure 1) where it was found that a phenolic (or analogous $-NH_2$) group was required for activity, as removal of this group resulted in complete loss of activity. It was also shown that simple phenols (with the exception of hydroquinones **6** and **7**) had much lower activity than **1**, suggesting that the indole moiety has significant importance, befitting of its place as a privileged structure.³⁵ Investigating different scaffolds yielded some interesting findings too, identifying compounds with improved activities to **1**, indicating that the NH group of the indole is not essential for activity, and that other aromatic systems can stabilise the phenoxy radical in addition to indole. Surprisingly, the *O*-substituted analogues showed higher activity than expected.

Overall, this approach has identified six new promising compounds (**14**, **16**, **18**, **19**, **20** and **22**) as superior fragments on which to base the design of new bioactives for glioblastoma, and future work will utilise these compounds as leads. A significant breadth of chemical space has been explored so far within this work, however the local chemical space of any of the active functional analogues of compound **1** has not been probed to any appreciable depth. Future work will therefore also focus on refining and developing the structures of these newly identified compounds in order to improve their activities and physicochemical properties via an in-depth SAR approach.

That said, glioblastoma is a very heterogeneous tumour, therefore one would expect different compounds to have different activities in different biological samples generated from it. As such, compounds that have similarly high activities against all (or most) of the cultures tested could in fact be highlighting structures that facilitate anti-proliferative activity via a universal mechanism which is independent of the genetic profile of the individual tumour. Such universally acting compounds would be much more useful in a clinical setting and would reduce the need for tumour profiling and patient stratification.

Experimental Section

BDE Calculations

DFT geometry optimisations of compounds and their corresponding radicals were carried out using the B3P86 functional,^{36, 37} previously revealed as effective in calculations of this type,^{24, 38} in conjunction with the 6-311+G(d,p) basis set.³⁹⁻⁴² The optimised structures were confirmed as real minima by vibrational frequency analysis (no imaginary frequencies) and zero-point energy (ZPE) corrections were obtained. The spin restricted open-shell (RODFT) approach was used for optimisation of the radical species. While restricted open shell calculations incorrectly prevent spin polarisation, there is no spin contamination as in unrestricted open shell calculations and the correct $\langle S^2 \rangle$ for the corresponding wavefunctions are obtained (i.e. 0.75 for radicals). The total enthalpy of a species X, $H(X)$, at temperature T (298.15 K) was calculated from the expression:

$$H(X) = E_{\text{SCF}} + \text{ZPE} + U + RT \quad \text{Eq. (1)}$$

where E_{SCF} is the electronic self-consistent field energy, ZPE is the zero-point energy, and U the combined translational, rotational and vibrational contributions. RT represents the PV-work term and is added to convert the energy to the enthalpy. Vibrational frequencies were used unscaled to obtain

the zero-point vibrational energies (ZPEs) and the vibrational contributions to the enthalpy. Using the total enthalpies, BDE values were determined as follows:

$$\text{BDE} = \text{H}(\text{RO}\cdot) + \text{H}(\text{H}\cdot) - \text{H}(\text{ROH}) \quad \text{Eq. (2)}$$

All the DFT calculations were performed Jaguar v9.0 (Schrodinger LLC, New York, NY, 2017)

Generic information

Reactions were followed by analytical thin layer chromatography (TLC) using plastic-backed TLC plates coated in silica G/UV₂₅₄, run in a variety of solvent systems and visualised with a UV light at 254 nm, *p*-anisaldehyde stain and/or potassium permanganate stain. Commercially available solvents and reagents were purchased from Fisher, Sigma Aldrich, TCI and Fluorochem and were used without further purification unless specified in the syntheses. Flash column chromatography was carried out on Davisil silica 60 Å (40 – 63 μm) under bellows pressure. High resolution mass spectra were obtained at the EPSRC UK National Mass Spectrometry Facility in Swansea University's College of Medicine using a LTQ Orbitrap XL™ Hybrid Ion Trap-Orbitrap Mass Spectrometer coupled to a TriVersa NanoMate® ESI source. Low resolution mass spectra were obtained on a Thermo Finnigan LCQ Advantage MAX using electrospray ionisation (ESI) or atmospheric pressure chemical ionisation (APCI). ¹H and ¹³C NMR were carried out on a Bruker Fourier 300 (300 MHz) or a Bruker Advance III 400 (400 MHz) with broad band decoupling, and all chemical shifts (δ) quoted in parts per million (ppm) relative to the residual solvent peaks of CHCl₃ (δ_H 7.26, δ_C 77.16) or *d*₅-DMSO (δ_H 2.50, δ_C 39.52). *J* values are given in Hertz (Hz). Infrared spectra were recorded on a solid sample using a Thermo Nicolet IR-200 FT-IR. Melting points are uncorrected, and were recorded using a Stuart SMP10. Preparative liquid chromatography was carried out on a Teledyne Isco CombiFlash® Rf 200. Elemental analysis was carried out using a Thermo Scientific™ FLASH 2000 CHNS/O Analyser. Petroleum ether refers to

the fraction that boils between 40-60 °C. Assignments of NMR spectra was aided with the use of DEPT-135, and in some cases HSQC and HMBC.

Compound synthesis

2-(1H-Indol-2-yl)phenol (**1**)⁴³

3-12, 17, 18, 21-23 and indole were purchased from Sigma-Aldrich, UK.

Compounds **14** and **15** were purchased from TCI Chemicals, UK.

2-(20-Methoxyphenyl)-1H-indole (**13**)³

2-(Naphthelen-7-yl) phenol (**16**)

To a flask containing water (5 mL), was added 2-bromonaphthalene (331 mg, 1.6 mmol), 2-hydroxyphenylboronic acid (500 mg, 2.4 mmol), diisopropylamine (DIPA, 0.45 mL, 3.2 mmol) and palladium (II) acetate (12.3 mg, 0.25 mol%). The reaction was heated to reflux for 3.5 hours, and was allowed to cool to room temperature before being diluted with brine (40 mL) and extracted with ethyl acetate (5 × 20 mL). The reaction was filtered through Celite®, and the filtrate dried (MgSO₄) and filtered. The crude reaction was purified *via* flash column chromatography on silica gel (5:1 petroleum ether: ethyl acetate) to afford the title compound as a pale yellow solid (288 mg, 82% yield). M.p. 93-96 °C; R_f = 0.37 (5:1 petroleum ether: ethyl acetate); ¹H NMR (300 MHz, CDCl₃): δ_H = 8.03-7.97 (2H, m, Ar), 7.96-7.88 (2H, m, Ar), 7.66-7.54 (3H, m, Ar), 7.43-7.30 (2H, m, Ar), 7.13 (2H, m, Ar), 5.42 (1H, s, OH); ¹³C NMR (75 MHz, CDCl₃): δ_C = 152.7 (Ar, C_q), 134.6 (Ar, C_q), 133.7 (Ar, C_q), 132.8 (Ar, C_q), 130.3 (Ar, CH), 129.4 (Ar, CH), 129.2 (Ar, CH), 128.2 (Ar, C_q), 128.1 (Ar, CH), 127.9 (Ar, CH), 127.9 (Ar, CH), 127.2 (Ar, CH), 126.7 (Ar, CH), 126.5 (Ar,

CH), 121.1 (Ar, CH), 116.0 (Ar, CH); IR (neat, cm^{-1}) ν = 3520 (OH stretch), 750 (Aromatic C-C bend); MS (EI): m/z 220 (M); HRMS found: $[\text{M}+\text{H}]^+$ 221.0960, $\text{C}_{16}\text{H}_{12}\text{O}+\text{H}^+$ requires 221.0961.

2-(1H-Indol-2-yl)-4-methylphenol (19)

Phenylhydrazine (108 mg, 1.00 mmol), 2-hydroxy-5-methylacetophenone (216 mg, 1.44 mmol) and *p*-toluenesulfonic acid (20 mg, 0.10 mmol) were heated under microwave irradiation at 200°C for 20 minutes. The crude reaction was purified *via* flash column chromatography on silica gel (5:1 petroleum ether: ethyl acetate) to afford the title compound as a dark solid (68 mg, 31% yield). R_f = 0.09 (5:1 petroleum ether: ethyl acetate); ^1H NMR (300 MHz, CDCl_3): δ_{H} = 9.28 (1H, br s, NH), 7.65 (1H, d, J = 8.0 Hz, Ar), 7.51 (1H, d, J = 1.5 Hz, Ar), 7.42 (1H, d, J = 8.0 Hz, Ar), 7.20 (1H, td, J = 7.5, 1.0 Hz, Ar), 7.13 (1H, td, J = 7.5, 1.0 Hz, Ar), 7.01 (1H, dd, J = 8.0, 2.0 Hz, Ar), 6.78 – 6.88 (2H, m, Ar), 5.43 (1H, br s, OH), 2.25 (3H, s, CH_3); ^{13}C NMR (100 MHz, CDCl_3): δ_{C} = 150.1 (C_q , Ar), 136.6 (C_q , Ar), 135.3 (C_q , Ar), 130.9 (C_q , Ar), 129.6 (CH, Ar), 128.7 (CH, Ar), 128.7 (C_q , Ar), 122.3 (CH, Ar), 120.6 (CH, Ar), 120.2 (CH, Ar), 119.0 (C_q , Ar), 116.6 (CH, Ar), 111.1 (CH, Ar), 100.2 (CH, Ar), 20.7 (CH_3); MS (EI): m/z 224 ($[\text{M}+\text{H}]^+$); HRMS found: $[\text{M}-\text{H}]^-$ 222.0924, $\text{C}_{15}\text{H}_{13}\text{NO}-\text{H}^+$ requires 222.0924.

2-(1H-Indol-3-yl)phenol (20)

2-Benzyloxyphenylacetic acid (983 mg, 4.06 mmol) was stirred in methanol (45 mL) and sulfuric acid (2 drops) at room temperature for 72 hours to yield methyl 2-(2-(benzyloxy)phenyl)acetate. R_f = 0.60 (3:1 petroleum ether: ethyl acetate); ^1H NMR (300 MHz, CDCl_3): δ_{H} = 7.45 – 7.29 (5H, m, Ar), 7.29 – 7.18 (2H, m, Ar), 6.94 (2H, m, Ar), 5.08 (2H, s, O- CH_2 -Ar), 3.70 (2H, s, Ar- CH_2 -COOMe), 3.64 (3H, s, CH_3).

The crude methyl ester was reduced to the alcohol by stirring in THF (dry, 15 mL) at 0°C and adding LiAlH_4 (308 mg, 8.11 mmol) under an atmosphere of nitrogen. The ice bath was then removed, and the reaction was stirred at room temperature for 90 minutes. The reaction was quenched

with NaOH_(aq) (10 mL, 0.1 M). The crude product was extracted with ethyl acetate (3 × 10 mL), and the combined organic layers were dried over MgSO₄ and filtered before being concentrated *in vacuo* to yield crude 2-(2-(benzyloxy)phenyl)ethanol. R_f = 0.22 (3:1 petroleum ether: ethyl acetate); ¹H NMR (300 MHz, CDCl₃): δ_H = 7.49 – 7.32 (5H, m, Ar), 7.28 – 7.19 (2H, m, Ar), 7.00 - 6.91 (2H, m, Ar), 5.10 (2H, s, Ar-CH₂-OAr), 3.87 (2H, t, *J* = 6.5, CH₂-OH), 2.98 (2H, t, *J* = 6.5 Hz, Ar-CH₂-CH₂OH), 1.95 (1H, br s, OH).

The crude alcohol was oxidised to the aldehyde by stirring with pyridinium chlorochromate (1.31 g, 6.08 mmol) in CH₂Cl₂ (40 mL) in the presence of crushed molecular sieves (650 mg) at room temperature for 22 hours. The solvent was removed *in vacuo*, and the crude reaction was dissolved in diethyl ether (40 mL), before being filtered through Celite®. The crude reaction was purified by flash column chromatography (19:1 petroleum ether: ethyl acetate) to yield 0.70 g of an 84:16 ratio of products, which included 468 mg (51% yield over 3 steps) of the major product 2-(2-(benzyloxy)phenyl)acetaldehyde. R_f = 0.61 (3:1 petroleum ether: ethyl acetate); ¹H NMR (300 MHz, CDCl₃): δ_H = 9.72 (1H, t, *J* = 2.0 Hz, CHO), 7.45 – 7.24 (6H, m, Ar), 7.20 - 7.14 (1H, m, Ar), 7.00 - 6.93 (2H, m, Ar), 5.08 (2H, s, O-CH₂-Ar), 3.70 (2H, d, *J* = 2.0 Hz, CH₂-CHO).

The mixture of aldehydes (0.70g, of which 468 mg, 2.07 mmol was the desired aldehyde) was added to a microwave vial with phenyl hydrazine (336 mg, 3.11 mmol) and *p*-toluenesulfonic acid (40 mg, 0.21 mmol) and heated at 200 °C for 20 minutes. The crude product was purified by flash column chromatography on silica gel (19:1 → 9:1 petroleum ether: ethyl acetate) to yield 3-(2-(benzyloxy)phenyl)-1*H*-indole (200 mg, 32% yield). ¹H NMR (300 MHz, CDCl₃): δ_H = 8.12 (1H, br s, NH), 7.95 (1H, d, *J* = 7.5 Hz, Ar), 7.79 (1H, dd, *J* = 7.5, 1.5 Hz, Ar), 7.53 (1H, d, *J* = 2.5 Hz, Ar), 7.42 – 7.11 (11H, m, Ar), 5.14 (2H, s, CH₂).

Methanol (10 mL) was added to a two-necked flask containing 3-(2-(benzyloxy)phenyl)-1*H*-indole (200 mg, 0.67 mmol) and palladium on carbon (20 mg, 10 wt%). The flask was evacuated and backfilled with nitrogen twice, before being evacuated and backfilled with hydrogen twice. The reaction was then stirred at room temperature under an atmosphere of hydrogen for 24 hours, and the

crude product was filtered through Celite® and purified by flash column chromatography on silica gel (4:1 → 3:1 petroleum ether: ethyl acetate) to yield 2-(1H-indol-3-yl)phenol (119 mg, 85% yield) as a thick orange oil. $R_f = 0.29$ (3:1 petroleum ether: ethyl acetate), 0.12 (4:1 petroleum ether: ethyl acetate); $^1\text{H NMR}$ (300 MHz, CDCl_3): $\delta_{\text{H}} = 8.31$ (1H, br s, NH), 7.73 (1H, d, $J = 8$ Hz, Ar), 7.50 (1H, dd, $J = 7.5, 1.5$ Hz, Ar), 7.45 – 7.31 (3H, m, Ar), 7.31 – 7.20 (2H, m, Ar), 7.19 – 7.08 (2H, m, Ar), 5.69 (1H, br s, OH); $^{13}\text{C NMR}$ (75 MHz, CDCl_3): $\delta_{\text{C}} = 153.2$ (Ar, C_q), 136.3 (Ar, C_q), 130.9 (Ar, CH), 128.6 (Ar, CH), 126.2 (Ar, C_q), 123.4 (Ar, CH), 122.9 (Ar, CH), 121.1 (Ar, C_q), 120.7 (Ar, CH), 120.5 (Ar, CH), 119.7 (Ar, CH), 115.5 (Ar, CH), 111.7 (Ar, CH); MS (ESI): m/z 208 ($[\text{M}-\text{H}]^-$); HRMS found: $[\text{M}+\text{H}]^+ 210.0913$, $\text{C}_{14}\text{H}_{11}\text{NO}+\text{H}^+$ requires 210.0913.

2-(Indolin-2-yl)phenol (24)

To a flask containing glacial acetic acid (10 mL) was added compound **1** (1.0 mmol, 209 mg) and sodium cyanoborohydride (12.0 mmol, 754 mg), and the reaction was stirred at room temperature for 26 hours. The crude reaction was then quenched by careful addition of water (100 mL), before adding solid sodium hydroxide to pH ~12. The crude reaction was extracted with ethyl acetate (3 × 20 mL), dried over MgSO_4 and filtered. The product was purified *via* flash column chromatography on silica gel (19:1 petroleum ether: ethyl acetate) to afford the title compound as a pale orange solid (92 mg, 43% yield). $R_f = 0.60$ (3:1 petroleum ether: ethyl acetate), 0.16 (19:1 petroleum ether: ethyl acetate); $^1\text{H NMR}$ (300 MHz, CDCl_3): $\delta_{\text{H}} = 9.75$ (1H, br s, OH), 7.28 – 7.10 (3H, m, Ar), 7.06 (1H, d, $J = 7.5$ Hz, Ar), 6.98 – 6.80 (4H, m, Ar), 4.92 (1H, dd, $J = 12.5, 8.5$ Hz, CH), 4.34 (1H, br s, NH), 3.38 – 3.04 (2H, m, CH_2); $^{13}\text{C NMR}$ (75 MHz, CDCl_3): $\delta_{\text{C}} = 156.88$ (C_q , Ar), 148.7 (C_q , Ar), 130.8 (C_q , Ar), 129.1 (CH, Ar), 128.5 (CH, Ar), 127.7 (CH, Ar), 124.9 (C_q , Ar), 124.8 (CH, Ar), 121.5 (CH, Ar), 119.5 (CH, Ar), 117.6 (CH, Ar), 112.0 (CH, Ar), 65.6 (CH), 38.4 (CH_2); MS (ESI): m/z 212 ($[\text{M}+\text{H}]^+$).

2-(1*H*-Indol-2-yl)phenyl benzoate (25)

Compound **1** (0.97 mmol, 202 mg), benzoyl chloride (1.16 mmol, 135 μ L), triethylamine (1.46 mmol, 203 μ L) and DMAP (0.1 mmol, 12 mg) was stirred in CH₂Cl₂ (10 mL) at room temperature for 18 hours. Upon completion by TLC, the crude reaction was washed with 1M HCl (2 \times 10 mL), water (10 mL) and brine (10 mL). The crude reaction was purified *via* preparative liquid chromatography on silica gel (19:1 to 9:1 petroleum ether: ethyl acetate) to afford the title product as a yellow solid (141 mg, 47% yield). M.p. 148 - 168 $^{\circ}$ C (decomposes); R_f = 0.18 (9:1 petroleum ether: ethyl acetate); ¹H NMR (300 MHz, CDCl₃): δ_{H} = 8.60 (1H, s, NH), 8.23 (2H, d, *J* = 7.5 Hz, Ar), 7.79 – 7.03 (11H, m, Ar), 6.83 (1H, s, Ar); ¹³C NMR (75 MHz, CDCl₃): δ_{C} = 165.2 (C=O), 147.7 (Ar, C_q), 136.5 (Ar, C_q), 134.1 (Ar, CH), 133.7 (Ar, C_q), 130.3 (Ar, CH), 129.3 (Ar, C_q), 129.1 (Ar, CH), 129.0 (Ar, CH), 128.8 (Ar, CH), 128.6 (Ar, C_q), 126.8 (Ar, CH), 125.9 (Ar, C_q), 123.8 (Ar, CH), 122.5 (Ar, CH), 120.8 (Ar, CH), 120.1 (Ar, CH), 111.0 (Ar, CH), 102.8 (Ar, CH); IR (neat, cm⁻¹) ν = 1725 (C=O stretch), 1260 (C-O stretch); MS (ESI): *m/z* 314 ([M+H]⁺); HRMS found: [M+H]⁺ 314.1184, C₂₁H₁₅NO₂+H requires 314.1176.

2-(1*H*-Indol-2-yl)phenyl acetate (26)

Compound **1** (101.7 mg, 0.59 mmol), acetyl chloride (46 μ L, 0.65 mmol), triethylamine (54 μ L) and DMAP (6 mg, 0.05 mmol) were added to CH₂Cl₂ (5 mL) and stirred at room temperature for 16 h. The reaction was washed with 1 M HCl (3 \times 5 mL), water (1 \times 5 mL) and brine (1 \times 5 mL), dried (MgSO₄), filtered and the solvent was removed *in vacuo*. The reaction was purified by flash column chromatography on silica gel (5:1 petroleum ether: ethyl acetate) to yield the title product as an off-white solid (84.3 mg, 71% yield). M.p. 112-127 $^{\circ}$ C; R_f = 0.23 (5:1 petroleum ether: ethyl acetate); ¹H NMR (300 MHz, CDCl₃): δ_{H} = 8.50 (1H, s, NH), 7.70-7.62 (2H, m, Ar), 7.43-7.32 (3H, m, Ar), 7.26-7.09 (3H, m, Ar), 6.78-6.82 (1H, m, Ar), 2.31 (3H, s, CH₃); ¹³C NMR (75 MHz, CDCl₃): δ_{C} = 169.4 (C=O), 147.6 (Ar), 136.6 (Ar), 133.9 (Ar), 129.3 (Ar), 128.9 (Ar), 128.7 (Ar), 126.8 (Ar), 125.9

(Ar), 123.7 (Ar), 122.7 (Ar), 120.9 (Ar), 120.3 (Ar), 111.0 (Ar), 102.7 (Ar), 21.4 (CH₃); IR (neat, cm⁻¹) ν = 3357 (N-H stretch), 1735 (C=O stretch), 1368 (aromatic C-C stretch), 1220 (C-O stretch); MS (ESI): m/z 252 ([M+H]⁺); HRMS found: [M+H]⁺ 252.1021, C₁₆H₁₃NO₂+H⁺ requires 252.1019.

2-(1*H*-Indol-2-yl)phenyl heptanoate (27)

Compound **1** (0.92 mmol, 192 mg), heptanoyl chloride (1.10 mmol, 171 μ L), triethylamine (1.38 mmol, 192 μ L) and DMAP (0.1 mmol, 12 mg) was stirred in CH₂Cl₂ (10 mL) at room temperature for 18 hours. Upon completion by TLC, the crude reaction was washed with 1M HCl (2 \times 10 mL), water (10 mL) and brine (10 mL). The crude reaction was purified *via* preparative liquid chromatography on silica gel (19:1 to 9:1 petroleum ether: ethyl acetate) to afford the title product as a yellow solid (225 mg, 76% yield). M.p. 51 - 54 °C; R_f = 0.15 (9:1 petroleum ether: ethyl acetate); ¹H NMR (300 MHz, CDCl₃): δ_{H} = 8.53 (1H, br s, NH), 7.70 – 7.61 (2H, m, Ar), 7.41 – 7.27 (3H, m, Ar), 7.25 – 7.10 (3H, m, Ar), 6.81 – 6.76 (1H, m, Ar), 2.59 (2H, t, J = 7.5 Hz, CH₂), 1.70 (2H, pent, J = 7.5 Hz, CH₂), 1.39 – 1.19 (6H, m, 3 \times CH₂), 0.87 (3H, t, J = 6.5 Hz, CH₃); ¹³C NMR (75 MHz, CDCl₃): δ_{C} = 172.4 (C=O), 147.6 (Ar, C_q), 136.5 (Ar, C_q), 134.0 (Ar, C_q), 129.4 (Ar, CH), 128.8 (Ar, CH), 128.7 (Ar, C_q), 126.7 (Ar, CH), 125.9 (Ar, C_q), 123.7 (Ar, CH), 122.6 (Ar, CH), 120.8 (Ar, CH), 120.2 (Ar, CH), 111.0 (Ar, CH), 102.6 (Ar, CH), 34.7 (CH₂), 31.5 (CH₂), 28.9 (CH₂), 24.9 (CH₂), 22.5 (CH₂), 14.1 (CH₃); IR (neat, cm⁻¹) ν = 1145 (C-O stretch), 1746 (C=O stretch), 2928 (C-H stretch); MS (ESI): m/z 322 ([M+H]⁺); HRMS found: [M+H]⁺ 322.1805, C₂₁H₂₃NO₂+H requires 322.1802.

SRB Assay Procedure

Short-term cell cultures (IN1472, IN1528, IN1760) were prepared from approximately 10mg of adult GBM biopsy tissue and maintained in Hams F10 nutrient mix [Invitrogen, Paisley UK] containing 10% foetal calf serum in a 37 °C non-CO₂ incubator as previously described.⁴⁴ Passages

of 10 to 14 were employed for the current study. In addition, we also employed U251 and U87 which are established GBM cell lines cultured under similar conditions.

Treated cells were assessed for their capacity to proliferate following treatment with compounds using a sulphorhodamine B (SRB) assay.⁴⁵ Briefly, 3000 cells were seeded per well in a 96 well plate and allowed to reach exponential growth (48 hours). Compounds were dissolved in DMSO [Sigma Aldrich; UK] and cells were treated for 72 hours with serial dilutions of the test compound. The culture medium was removed and the cells fixed in 10% trichloroacetic acid [Sigma Aldrich; UK] on ice for 30 min followed by washing in water and air-drying. Cells were stained with 0.4% sulforhodamine B [Sigma Aldrich; UK] prepared in 1% acetic acid for 15-20 mins, washed in 1% acetic acid and air-dried. The dye was solubilized in 100 μ L of 10mM Tris (not buffered) and read at 560nm [Dynatech MR5000] for quantification.

Analysis was performed using Sigmoidal Dose Response (Variable Slope) (Non-Linear Fit).

Conflicts of interest

There are no conflicts of interest to declare.

Acknowledgements

The authors would like to thank the Sydney Driscoll Neuroscience Foundation and Brain Tumour North West for funding. Thanks also goes to the EPSRC UK National Mass Spectrometry Facility (NMSF), Swansea for accurate mass measurements.

References

1. A. Brodbelt, D. Greenberg, T. Winters, M. Williams, S. Vernon, V. P. Collins and N. Natl Canc Information, *European Journal of Cancer*, 2015, **51**, 533-542.
2. R. Stupp, W. P. Mason, M. J. van den Bent, M. Weller, B. Fisher, M. J. B. Taphoorn, K. Belanger, A. A. Brandes, C. Marosi, U. Bogdahn, J. Curschmann, R. C. Janzer, S. K. Ludwin, T. Gorlia, A. Allgeier, D. Lacombe, J. G. Cairncross, E. Eisenhauer, R. O. Mirimanoff, D. Van Den Weyngaert, S. Kaendler, P. Krauseneck, N. Vinolas, S. Villa, R. E.

Wurm, M. H. B. Maillot, F. Spagnolli, G. Kantor, J. P. Malhaire, L. Renard, O. De Witte, L. Scandolaro, C. J. Vecht, P. Maingon, J. Lutterbach, A. Kobierska, M. Bolla, R. Souchon, C. Mitine, T. Tzuk-Shina, A. Kuten, G. Haferkamp, J. de Greve, F. Priou, J. Menten, I. Rutten, P. Clavere, A. Malmstrom, B. Jancar, E. Newlands, K. Pigott, A. Twijnstra, O. Chinot, M. Reni, A. Boiardi, M. Fabbro, M. Campone, J. Bozzino, M. Frenay, J. Gijtenbeek, A. A. Brandes, J. Y. Delattre, U. Bogdahn, U. De Paula, M. J. van den Bent, C. Hanzen, G. Pavanato, S. Schraub, R. Pfeffer, R. Soffiatti, M. Weller, R. D. Kortmann, M. Taphoorn, J. L. Torrecilla, C. Marosi, W. Grisold, P. Huget, P. Forsyth, D. Fulton, S. Kirby, R. Wong, D. Fenton, B. Fisher, G. Cairncross, P. Whitlock, K. Belanger, S. Burdette-Radoux, S. Gertler, S. Saunders, K. Laing, J. Siddiqui, L. A. Martin, S. Gulavita, J. Perry, W. Mason, B. Thiessen, H. Pai, Z. Y. Alam, D. Eisenstat, W. Mingrone, S. Hofer, G. Pesce, J. Curschmann, P. Y. Dietrich, R. Stupp, R. O. Mirimanoff, P. Thum, B. Baumert, G. Ryan and B. European Org Res Treatment Canc, *N. Engl. J. Med.*, 2005, **352**, 987-996.

3. S. Prabhu, Z. Akbar, F. Harris, K. Karakoula, R. Lea, F. Rowther, T. Warr and T. Snape, *Bioorg. Med. Chem.*, 2013, **21**, 1918-1924.
4. In-house *in vitro* blood-brain-barrier model (WO2018020274 (A1)) showed compound **1** to be a highly permeable compound.
5. J. S. Wright, E. R. Johnson and G. A. DiLabio, *J. Am. Chem. Soc.*, 2001, **123**, 1173-1183.
6. M. Leopoldini, T. Marino, N. Russo and M. Toscano, *J. Phys. Chem. A*, 2004, **108**, 4916-4922.
7. D. Farmanzadeh and M. Najafi, *Struct. Chem.*, 2015, **26**, 831-844.
8. L. Chin, M. Meyerson, K. Aldape, D. Bigner, T. Mikkelsen, S. VandenBerg, A. Kahn, R. Penny, M. L. Ferguson, D. S. Gerhard, G. Getz, C. Brennan, B. S. Taylor, W. Winckler, P. Park, M. Ladanyi, K. A. Hoadley, R. G. W. Verhaak, D. N. Hayes, P. T. Spellman, D. Absher, B. A. Weir, L. Ding, D. Wheeler, M. S. Lawrence, K. Cibulskis, E. Mardis, J. H. Zhang, R. K. Wilson, L. Donehower, D. A. Wheeler, E. Purdom, J. Wallis, P. W. Laird, J. G. Herman, K. E. Schuebel, D. J. Weisenberger, S. B. Baylin, N. Schultz, J. Yao, R. Wiedemeyer, J. Weinstein, C. Sander, R. A. Gibbs, J. Gray, R. Kucherlapati, E. S. Lander, R. M. Myers, C. M. Perou, R. McLendon, A. Friedman, E. G. Van Meir, D. J. Brat, G. M. Mastrogiannakis, J. J. Olson, N. Lehman, W. K. A. Yung, O. Bogler, M. Berger, M. Prados, D. Muzny, M. Morgan, S. Scherer, A. Sabo, L. Nazareth, L. Lewis, O. Hall, Y. M. Zhu, Y. R. Ren, O. Alvi, J. Q. Yao, A. Hawes, S. Jhangiani, G. Fowler, A. San Lucas, C. Kovar, A. Cree, H. Dinh, J. Santibanez, V. Joshi, M. L. Gonzalez-Garay, C. A. Miller, A. Milosavljevic, C. Sougnez, T. Fennell, S. Mahan, J. Wilkinson, L. Ziaugra, R. Onofrio, T. Bloom, R. Nicol, K. Ardlie, J. Baldwin, S. Gabriel, R. S. Fulton, M. D. McLellan, D. E. Larson, X. Q. Shi, R. Abbott, L. Fulton, K. Chen, D. C. Koboldt, M. C. Wendl, R. Meyer, Y. Z. Tang, L. Lin, J. R. Osborne, B. H. Dunford-Shore, T. L. Miner, K. Delehaunty, C. Markovic, G. Swift, W. Courtney, C. Pohl, S. Abbott, A. Hawkins, S. Leong, C. Haipek, H. Schmidt, M. Wiechert, T. Vickery, S. Scott, D. J. Dooling, A. Chinwalla, G. M. Weinstock, M. O'Kelly, J. Robinson, G. Alexe, R. Beroukhim, S. Carter, D. Chiang, J. Gould, S. Gupta, J. Korn, C. Mermel, J. Mesirov, S. Monti, H. Nguyen, M. Parkin, M. Reich, N. Stransky, L. Garraway, T. Golub, A. Protopopov, I. Perna, S. Aronson, N. Sathiamoorthy, G. Ren, H. Kim, S. K. Kong, Y. H. Xiao, I. S. Kohane, J. Seidman, L. Cope, F. Pan, D. Van Den Berg, L. Van Neste, J. M. Yi, J. Z. Li, A. Southwick, S. Brady, A. Aggarwal, T. Chung, G. Sherlock, J. D. Brooks, L. R. Jakkula, A. V. Lapuk, H. Marr, S. Dorton, Y. G. Choi, J. Han, A. Ray, V. Wang, S. Durinck, M. Robinson, N. J. Wang, K. Vranizan, V. Peng, E. Van Name, G. V. Fontenay, J. Ngai, J. G. Conboy, B. Parvin, H. S. Feiler, T. P. Speed, N. D.

- Socci, A. Olshen, A. Lash, B. Reva, Y. Antipin, A. Stukalov, B. Gross, E. Cerami, W. Q. Wang, L. X. Qin, V. E. Seshan, L. Villafania, M. Cavatore, L. Borsu, A. Viale, W. Gerald, M. D. Topal, Y. Qi, S. Balu, Y. Shi, G. Wu, M. Bittner, T. Shelton, E. Lenkiewicz, S. Morris, D. Beasley, S. Sanders, R. Sfeir, J. Chen, D. Nassau, L. Feng, E. Hickey, C. Schaefer, S. Madhavan, K. Buetow, A. Barker, J. Vockley, C. Compton, J. Vaught, P. Fielding, F. Collins, P. Good, M. Guyer, B. Ozenberger, J. Peterson, E. Thomson, *Nature*, 2008, **455**, 1061-1068.
9. R. G. W. Verhaak, K. A. Hoadley, E. Purdom, V. Wang, Y. Qi, M. D. Wilkerson, C. R. Miller, L. Ding, T. Golub, J. P. Mesirov, G. Alexe, M. Lawrence, M. O'Kelly, P. Tamayo, B. A. Weir, S. Gabriel, W. Winckler, S. Gupta, L. Jakkula, H. S. Feiler, J. G. Hodgson, C. D. James, J. N. Sarkaria, C. Brennan, A. Kahn, P. T. Spellman, R. K. Wilson, T. P. Speed, J. W. Gray, M. Meyerson, G. Getz, C. M. Perou, D. N. Hayes, *Cancer cell*, 2010, **17**, 98-110.
 10. R. Stupp, M. E. Hegi, W. P. Mason, M. J. van den Bent, M. J. B. Taphoorn, R. C. Janzer, S. K. Ludwin, A. Allgeier, B. Fisher, K. Belanger, P. Hau, A. A. Brandes, J. Gijtenbeek, C. Marosi, C. J. Vecht, K. Mokhtari, P. Wesseling, S. Villa, E. Eisenhauer, T. Gorlia, M. Weller, D. Lacombe, J. G. Cairncross, R. O. Mirimanoff, *Lancet Oncology*, 2009, **10**, 459-466.
 11. M. D. Blough, D. C. Beauchamp, M. R. Westgate, J. J. Kelly and J. G. Cairncross, *J. Neuro-Oncol*, 2011, **102**, 1-7.
 12. B. Murnyak, M. C. Kouhsari, R. Hershkovitch, B. Kalman, G. Marko-Varga, A. Klekner and T. Hortobagyi, *Oncotarget*, 2017, **8**, 46348-46362.
 13. N. Gaspar, L. Marshall, L. Perryman, D. A. Bax, S. E. Little, M. Viana-Pereira, S. Y. Sharp, G. Vassal, A. D. J. Pearson, R. M. Reis, D. Hargrave, P. Workman and C. Jones, *Cancer Res.*, 2010, **70**, 9243-9252.
 14. N. Potter, S. Ashmore, K. Karakoula, S. Ward, B. Suarez-Merino, M. Luxsuwong, D. G. Thomas, J. Darling and T. Warr, *Neuro-Oncol.*, 2010, **12**, 67-67.
 15. H. M. Sun, G. Tawa and A. Wallqvist, *Drug Discovery Today*, 2012, **17**, 310-324.
 16. L. H. Yao, Y. M. Jiang, J. Shi, F. A. Tomas-Barberan, N. Datta, R. Singanusong and S. S. Chen, *Plant Foods Hum Nutr*, 2004, **59**, 113-122.
 17. J. Dai and R. J. Mumper, *Molecules*, 2010, **15**, 7313-7352.
 18. E. I. Parkinson and P. J. Hergenrother, *Acc. Chem. Res.*, 2015, **48**, 2715-2723.
 19. R. W. Owen, A. Giacosa, W. E. Hull, R. Haubner, B. Spiegelhalder and H. Bartsch, *European Journal of Cancer*, 2000, **36**, 1235-1247.
 20. C. A. Gomes, T. G. da Cruz, J. L. Andrade, N. Milhazes, F. Borges and M. P. M. Marques, *J. Med. Chem.*, 2003, **46**, 5395-5401.
 21. C. C. Winterbourn, *Nat. Chem. Biol.*, 2008, **4**, 278-286.
 22. V. E. Kagan, A. I. Kuzmenko, A. A. Shvedova, E. R. Kisin, R. Li, I. Martin, P. J. Quinn, V. A. Tyurin, Y. Y. Tyurina and J. C. Yalowich, *Biochim. Biophys. Acta.*, 2003, **1620**, 72-84.
 23. A. J. Javan and M. J. Javan, *Food Chemistry*, 2014, **165**, 451-459.

24. P. Trouillas, P. Marsal, D. Siri, R. Lazzaroni and J. L. Duroux, *Food Chemistry*, 2006, **97**, 679-688.
25. H. Y. Zhang, Y. M. Sung and X. L. Wang, *Chem. Eur. J.*, 2003, **9**, 502-508.
26. R. M. B. dos Santos and J. A. M. Simoes, *J. Phys. Chem. Ref. Data*, 1998, **27**, 707-739.
27. A. Rybina, B. Thaler, R. Kramer and D. P. Herten, *Phys. Chem. Chem. Phys.*, 2014, **16**, 19550-19555.
28. C. Jiang, S. Garg and T. D. Waite, *Environ. Sci. Technol.*, 2015, **49**, 14076-14084.
29. R. P. Sheridan and S. K. Kearsley, *Drug Discovery Today*, 2002, **7**, 903-911.
30. J. J. Irwin and B. K. Shoichet, *J. Chem. Inf. Model.*, 2005, **45**, 177-182.
31. M. J. Vainio, J. S. Puranen and M. S. Johnson, *J. Chem. Inf. Model.*, 2009, **49**, 492-502.
32. J. S. Puranen, M. J. Vainio and M. S. Johnson, *Journal of Computational Chemistry*, 2010, **31**, 1722-1732.
33. S. Suzen, P. Bozkaya, T. Coban and D. Nebioglu, *J. Enzyme Inhib. Med. Chem.*, 2006, **21**, 405-411.
34. T. Satoh and M. Hosokawa, *Annu. Rev. Pharmacol. Toxicol.*, 1998, **38**, 257-288.
35. F. R. D. Alves, E. J. Barreiro and C. A. M. Fraga, *Mini-Rev. Med. Chem.*, 2009, **9**, 782-793.
36. A. D. Becke, *J. Chem. Phys.*, 1993, **98**, 5648-5652.
37. J. P. Perdew, *Phys. Rev. B*, 1986, **33**, 8822-8824.
38. P. Kosinova, F. Di Meo, E. H. Anouar, J. L. Duroux and P. Trouillas, *Int. J. Quantum Chem.*, 2011, **111**, 1131-1142.
39. T. Clark, J. Chandrasekhar, G. W. Spitznagel and P. V. Schleyer, *Journal of Computational Chemistry*, 1983, **4**, 294-301.
40. M. J. Frisch, J. A. Pople and J. S. Binkley, *J. Chem. Phys.*, 1984, **80**, 3265-3269.
41. R. Krishnan, J. S. Binkley, R. Seeger and J. A. Pople, *J. Chem. Phys.*, 1980, **72**, 650-654.
42. A. D. McLean and G. S. Chandler, *J. Chem. Phys.*, 1980, **72**, 5639-5648.
43. T. J. Snape, *Synlett*, 2008, 2689-2691.
44. G. M. Lewandowicz, B. Harding, W. Harkness, R. Hayward, D. G. T. Thomas and J. L. Darling, *Eur. J. Cancer*, 2000, **36**, 1955-1964.
45. W. Voigt, in *Methods in Molecular Medicine*, 2005, vol. 110, pp. 39-48.